

# Understanding dose correction for high-resolution 50 kV electron-beam lithography on thick resist layers

Mattias Åstrand<sup>\*</sup>, Thomas Frisk, Hanna Ohlin, Ulrich Vogt

KTH Royal Institute of Technology, Department of Applied Physics, Biomedical and X-ray Physics, Albanova University Center, 106 91 Stockholm, Sweden

## ARTICLE INFO

### Keywords:

Nanofabrication  
Electron-beam lithography  
Proximity effect correction  
Chemically semi-amplified resist

## ABSTRACT

Electron-beam lithography (EBL) is a relevant technique to the nanoscience community as it enables the production of precise structures at the nanoscale. When writing features in a thick resist layer, dose insufficiency is typically encountered when resolution approaches the focal spot of the electron beam itself. We present a study of this phenomenon, a theory for its understanding and compensation, and a method for the assignment of the correct area dose for writing small features. Dose insufficiency originates from the proximity effect distributing energy in volumes of resist that are larger than intended. Based on a simple interpretation of the spread, a proximity effect correction (PEC) algorithm was established. Implementing this, we could realize high-quality nanostructures with direct-write 50 kV EBL on AR-P 6200 (CSAR 62) resist. The latter translates to quick and inexpensive exposures that offer good compatibility with further processes.

## 1. Introduction

Electron-beam lithography (EBL) is a well established tool within nanofabrication. It enables the patterning of nanometer-sized features without the necessity for a mask, meaning that it is both high resolution and versatile [1,2]. In EBL a resist layer is exposed to a beam of electrons; energy is deposited in the layer as a consequence of electron scattering and structural changes in the resist arise, altering its solubility properties. The angle of forward scattering of primary beam electrons is small and results in a conical write operation through the resist. Back-scattering in the resist material is rare and is more likely to happen in the substrate, should this be more dense. When it occurs, energetic electrons are scattered into neighbouring regions to the directly exposed resist area. The unintended exposure inevitably yields a decrease in resolution; this, together with broadening from forward scattered electrons, is referred to as the proximity effect [2]. To obtain appropriately dosed and sized features, proximity effect correction (PEC) schemes have been developed. These take into account the point spread function (PSF) of electrons through a resist layer, and suggest dose allocations and modifications to the starting pattern that is defined by the user [3–7].

When exposing a resist on a thin membrane (of, e.g., Si<sub>3</sub>N<sub>4</sub>), the detrimental effect of back-scattering may be eliminated [8]. The main limitation to high quality patterning is then forward scattering. The thicker the resist layer, the more apparent the broadening of the PSF and

thus the cone of exposure that comes with scattering of primary electrons. As a result, exposed features are certainly larger than the beam size. Accordingly, higher resist thicknesses demand the implementation of a “bias” to downsize to-be-written patterns; such a parameter works around beam broadening by preventing the collapse of features in dense patterns [9]. Thanks to the biasing of patterns, the ability to produce features that are close to their intended dimensions follows. Direct-writing through thick resist layers then enables the production of high aspect ratio (AR) resist nanostructures, and these may be implemented in plating molds or etch masks.

There are other process parameters that have a significant influence on EBL. Starting from the lithography tool, a high acceleration voltage is often chosen to reduce the effects of broadening due to scattering [2]. For lower voltages, scattering is promoted, meaning that dose is allocated more efficiently and exposures run faster, even though at lower resolution due to more broadening. An optimum may be found to ensure high resolution and fast writing. The resist type also plays an important role; to make an appropriate choice, one can recur to evaluating alternatives in terms of some figures of merit. The ability of a resist to react with little dose and provide complete write-through upon development is known as sensitivity. Another relevant figure is contrast, which translates to how wide the range of dose is for going from zero to full write-through. Usually, proficiency in one means lacking in the other, albeit chemically-amplified resists (CARs) have been designed to offer

<sup>\*</sup> Corresponding author.

E-mail address: [maastra@kth.se](mailto:maastra@kth.se) (M. Åstrand).

<https://doi.org/10.1016/j.mne.2022.100141>

Received 26 February 2022; Received in revised form 4 April 2022; Accepted 14 April 2022

Available online 20 April 2022

2590-0072/© 2022 The Authors. Published by Elsevier B.V. This is an open access article under the CC BY license (<http://creativecommons.org/licenses/by/4.0/>).

impressive numbers for both [10].

In this paper we report on a PEC model for writing on thick resist layers at the tool's resolution limit and in the absence of backscattering. It was observed that area elements, e.g., paths and polygons, that width-wise approach this limit tend to suffer from a dose insufficiency. We present an explanation for this phenomenon, stemming from a simplified interpretation of the PSF, and demonstrate an easy method for calculating the appropriate dose for small patterns. Structures with sub-100 nm features were fabricated by direct-write EBL on 410 nm AR-P 6200 resist (commonly referred to as CSAR 62) on  $\text{Si}_3\text{N}_4$  membranes with a 50 kV electron-beam (e-beam) system. CSAR 62 was implemented for its chemically semi-amplified nature and for its high plasma etch resistance, as compared to non-CAR alternatives like PMMA [11,12]. Developing a robust EBL procedure with such acceleration voltage and CAR-type resist yields a twofold advantage in terms of processing speed, and thus cost-efficiency, and opens the door to various subsequent processing steps like lift-off, dry etching or electroplating.

## 2. Method

The processing scheme that was followed in the laboratory is illustrated in Fig. 1. The implemented steps are explained in more detail in the subsections below.

### 2.1. Sample preparation

Samples were prepared on  $7.5 \times 7.5 \text{ mm}^2$ , 200 frame Si substrate chips (Silson, UK), equipped with 100 nm thick,  $250 \times 250 \mu\text{m}^2$   $\text{Si}_3\text{N}_4$

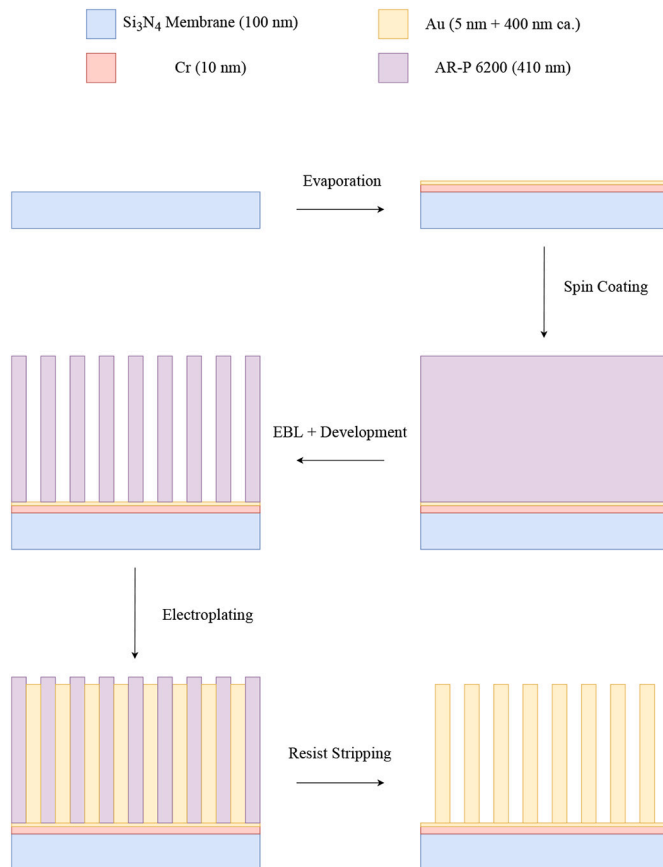


Fig. 1. Step-by-step visualisation of the nanofabrication process that was implemented for the realisation of high resolution structures. (For interpretation of the references to colour in this figure legend, the reader is referred to the web version of this article.)

membranes (blue layer in Fig. 1).

A thin metal seed layer for electroplating was grown on top of the chips: 10 nm chromium and 5 nm gold (red and yellow in Fig. 1, respectively) were evaporated in a UHV e-gun deposition system (Thermionics, US). Chromium served as an adhesion layer to gold, which was the actual plating seed layer. Note that, for the highest resolution results, we chose to study gold features that followed the EBL patterning by electroplating post-EBL openings in the resist, as opposed to imaging the resist directly with a scanning electron microscope (SEM). The latter was avoided to prevent unnecessary structural damages, given the electron-sensitive nature of the resist itself.

The resist layer was deposited by spin-coating of the chips with AR-P 6200.13 (AllResist, Germany; purple in Fig. 1). 50  $\mu\text{L}$  of adhesion promoter (AR 300–80 by AllResist – providing better adhesion of the resist to the metal-evaporated chips) were pipetted and spun on the chips at a rate of 4300 rpm for 60 s. Subsequently, 75  $\mu\text{L}$  of AR-P 6200.13 were also pipetted and spun on the chips at 4300 rpm for 60 s. Both spin-coating procedures were followed by baking on a 190 °C hotplate for 60 s. 410 nm CSAR 62 layers were thus obtained, and their thicknesses were evaluated by mechanically removing the resist in some area of the chips and performing contact profilometry with a surface profiler (KLA Tencor P-7, US).

### 2.2. Electron beam lithography – Design and process

The tool that was used for EBL was a 50 kV acceleration voltage system (VOYAGER, Raith GmbH, Germany); the column was operated in low current mode (30  $\mu\text{m}$  aperture size) for highest resolution. Exposure calibration started with acquiring a preliminary focus and correcting astigmatism by running a script that relied on the imaging of cylindrical test structures. Next, the e-beam current was measured with an on-holder Faraday cup, and patterning parameters (dwell time and speed) were calculated according to the current and the envisioned e-beam dose per area element. For the calculation to go through, some parameters were fixed: the e-beam exposure step size (SS) and line size (LS) were both set to 5 nm to match the known e-beam focus and yield no overlap in the two-dimensional grid of exposure. This was done for convenience as it established a direct relation between the focusing of the VOYAGER and the allocation of dose throughout the exposure area, which occurs by raster scans with write lines (WLs) that are LS wide and made up by spots that are SS in footprint, as shown in Fig. 2. Subsequent calculations and result visualisation becomes straightforward.

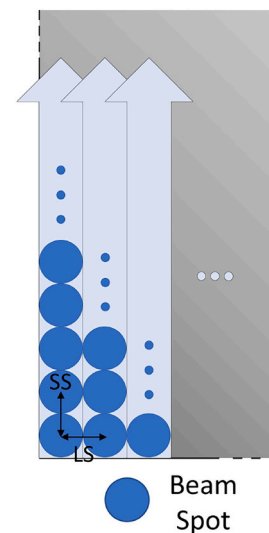


Fig. 2. Visualization of the beam spot allocation scheme throughout a to-be-patterned area. Beam spots are separated according to a step and a line size (SS and LS, respectively).

The base dose was given a relevant digit in  $\mu\text{C}/\text{cm}^2$ , and was modulated by multiplication with a dose factor wherever ramp up was necessary in patterning. Finally, stitching errors were minimised for the  $500 \times 500 \mu\text{m}^2$  write fields by a script that followed imaging of repeating, chess mat-like structures on the sample holder. This ensured nm fidelity in the placement of structures throughout a chip.

For patterning, chips were mounted to the VOYAGER holder with two nonadjacent clips, and three-point alignment schemes were implemented to account for any remaining tilt. This granted an even focus throughout the surfaces and thus uniform exposure of the resist layers on the chips. The write operation was in accordance with fully automated position lists that allocated patterns to the resist-on-membrane regions of the chips as defined in MATLAB with the Raith\_GDSII toolbox [13]. The implemented patterns consisted of gratings with 1:1 line-to-space ratio and line width on the order of a few tens of nm. Grating lines were either full or subdivided into 500 nm segments, with 50 nm vertical separation, and arranged in  $20 \times 20 \mu\text{m}^2$  arrays. Direct width reduction by the bias parameter (input to the MATLAB pattern generator) allowed for studying the appropriate area dose for write-through of intended line sizes.

As depicted in Fig. 3, the scaling of patterns by biasing eventually becomes an issue for the allocation of the correct area dose when there are only a few WLs left. The loss of a WL was identified as a critical phenomenon, and the underdose that followed from it was investigated by attempting to write grating lines accommodating different WL counts. Specifically, one, two, three, four, five and seven WL grating lines were designed and patterned, these too split into 500 nm segments, and arranged in  $20 \times 20 \mu\text{m}^2$  arrays.

Biasing was thus implemented both for the possibility to compensate for beam broadening, and thus realize features of the intended width, and to understand the dose loss phenomenon that is related to WL losses. Biasing was pushed to the limit, eventually leading to writing rectangular segments to which a single WL would be allocated by the VOYAGER. This was compared to the in principle equivalent action of writing with a single pixel line (SPL) of corresponding line-dose. The resolution limit of the resist layer thickness, in combination with the acceleration voltage of the EBL system, was thus put to the test by designing and patterning gratings of segments consisting of rectangles that are only one WL wide, and, alternatively, of segments that consisted of only one SPL. Both of these segment types were 500 nm long, and arranged in  $20 \times 20 \mu\text{m}^2$  arrays.

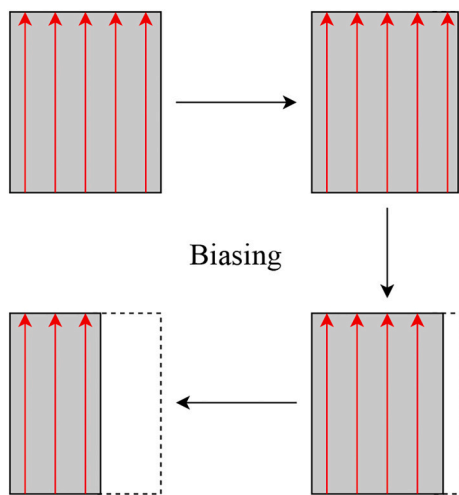


**Fig. 3.** Illustration of the effect of implementing a bias on the width of EBL patterns. The loss of WLs (red) follows from the downscaling of the area of exposure (grey). (For interpretation of the references to colour in this figure legend, the reader is referred to the web version of this article.)

### 2.3. Sample evaluation

Once e-beam exposure was complete, samples were developed in AR 600–546 (AllResist GmbH, Germany) for 60 s. The development was stopped with a 10 s dip in isopropanol and the samples were rinsed in n-pentane for 15 s. This was done at room temperature. Different samples were produced for the following series of results: evaluating the effect of bias; understanding that dose insufficiency is coupled to WL count; showcasing knowledge in appropriate dosage per area element; studying a one WL area element and comparing it to a SPL.

Pre-plating, a reactive ion etching (RIE) step was implemented for the removal of resist residues at the bottom of write-through regions [14]. For this, an Oxford Plasma Technology Plasmalab 80+ Reactive Ion Etch system was operated in RIE mode; etching was carried out for 15 s with the RIE RF generator driven at 50 W, with 10 sccm of  $\text{O}_2$  and a process pressure of  $8.5 \cdot 10^{-9}$  Torr. Direct current electroplating of gold was then performed in a sulphite-based gold bath [15]. Finally, the resist masks were stripped from the chips with the above system operated in RIE with inductively coupled plasma (ICP) mode. The process was carried out for 15 min, driving the RIE and ICP RF generators at 50 W and 250 W, respectively, with 20 sccm of  $\text{O}_2$  and a process pressure of  $7.5 \cdot 10^{-9}$  Torr. The obtained samples were imaged in a SEM (FEI Nova 200).

## 3. Results and discussion

### 3.1. Overcoming backscattering

As previously mentioned, an assumption that allows us to solely focus on forward scattering is that there is negligible backscattering from the substrate. To consolidate this, Fig. 4 is provided: a grating of dimensions  $20 \times 20 \mu\text{m}^2$  presents no evidence of uneven exposure of grating lines. Had backscattering played a role, it would have been highlighted by a difference in exposure in the central region as compared to peripheral areas. This is because of dose contributions by backscattered electrons from adjacent exposure sites. On bulk silicon, this effect should be visible within radii of  $1 \mu\text{m}$  (as expected from Monte Carlo simulations [16]), hence the dimensions in Fig. 4 are appropriate for evaluating backscattering in our samples. The absence of the latter means that forward scattering is indeed the only type of scattering that contributes towards the allocation of dose in our experiments.

### 3.2. Observing dose insufficiency

Resist documentation typically provides area doses at which

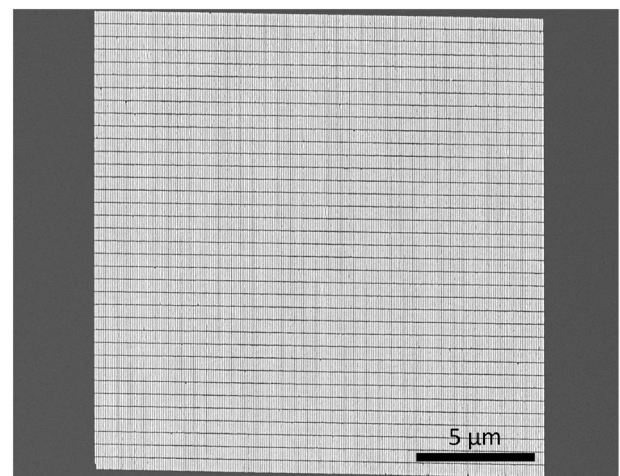


**Fig. 4.**  $20 \times 20 \mu\text{m}^2$  grating of 40 nm (intended) Au lines. EBL line segments were biased by 15 nm, hence the actual line width was of 25 nm, and 5 WLs were used for the exposure; the area dose was  $275 \mu\text{C}/\text{cm}^2$ .

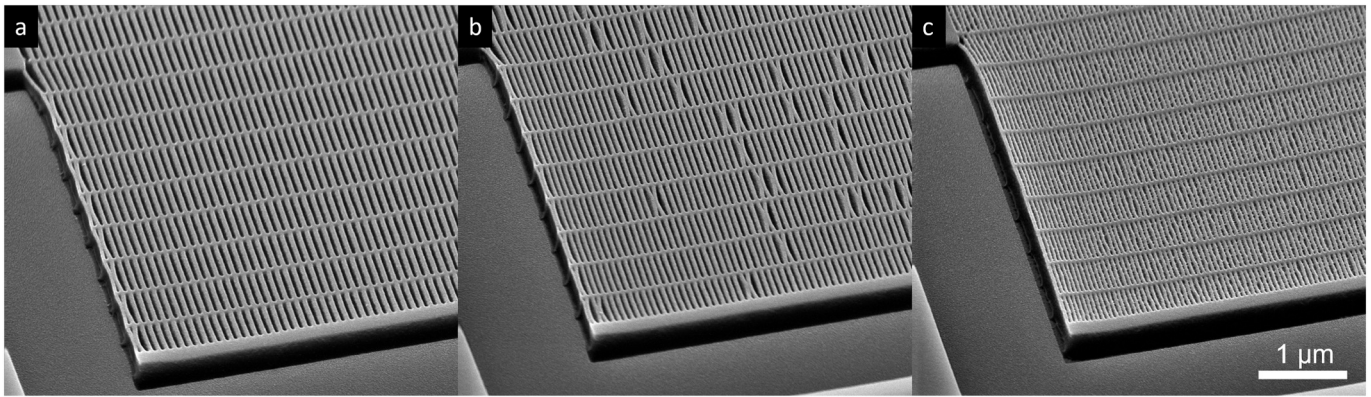


**Fig. 5.** Gratings of reducing period exposed by the same area dose of  $230 \mu\text{C}/\text{cm}^2$  as written on 410 nm CSAR 62. All exposures are biased by 15 nm to achieve a line-to-space ratio of 1. The period is of 100 nm in (a), 80 nm in (b) and 60 nm in (c).

exposure should be carried out to achieve write-through on a resist layer of given thickness. What is not addressed is whether such dose is capable of writing features of any width through such resist. Fig. 5 illustrates this issue by showcasing the inappropriateness of the area dose  $230 \mu\text{C}/\text{cm}^2$  for writing gratings of sub-100 nm period if no exposure parameters are changed. This dose had previously been observed to be appropriate for structures of approximately 100 nm in width through just over 400 nm CSAR 62 by other in-house studies. Clearly, the dose was not sufficient for writing 80 nm period gratings, and even more so for 60 nm ones, when a bias of 15 nm was implemented. The insufficiency has to stem from the only difference in the gratings in Fig. 5: the width of the lines that are written.

To support the above statement, Fig. 6 is provided, in which further attempts to achieve write-through for a period of 60 nm are shown. For these, dose was fixed at a higher value than in Fig. 5 (c), knowing that this would certainly not achieve write-through of patterns. Line width was decreased in steps of 2 nm by cutting off 1 nm on each side of the grating lines. Virtually no difference could be spotted for the exposure of 12 nm (a) and 10 nm (b) biased grating lines, whilst 8 nm lines appeared as clearly underdosed. Knowing that LS was fixed at 5 nm in our exposures, we can draw the conclusion that Fig. 6 (a) and (b) correspond to writing a 60 nm period grating with two WLs allocated per line, whilst Fig. 6 (c) corresponds to an attempt at realising the same grating, but with one WL per grating line only.

Even though biasing has to be implemented to sustain the down-scaling of features and periods in patterns, it inevitably yields a reduction in the WLs that are allocated per feature. A reduced number of WLs may not provide enough electrons for a complete write-through,

meaning that a dose ramp-up scheme is necessary for a successful EBL exposure.

### 3.3. Dose as a function of WL count

A question that arises is how to determine the dose that is appropriate for a given feature. From the above, the simple yet powerful interpretation of dose insufficiency originating from a reduced WL count follows, and a deeper understanding is gained by recalling Fig. 2 and reflecting on the meaning of area dose. When operating the VOYAGER, patterning parameters are input before actually specifying what patterns are to be written. Having SS and LS fixed, a unit for area is conceptually spanned, and this is used in calculations by the tool to translate dose to dwell time per beam spot according to current. If the dwell time is fixed prior to pattern definition, patterns that accommodate fewer WLs inevitably obtain less dose. If one assumes that dose is evenly split amongst the WLs that are allocated for writing a feature, the dose deficiency that is tied to losing a WL is easily calculated, and the ramp-up that is necessary to account for the WL loss is as expressed in Eq. (1), where #WL indicates WL count.

$$\text{Dose}(\#\text{WL} - 1) = \text{Dose}(\#\text{WL}) \cdot \left(1 + \frac{1}{\#\text{WL}}\right) \quad (1)$$

If the dose is spread across #WL, the dose per WL is  $1/\#\text{WL}$ . If one WL is removed, it follows that the dose that has been removed from the exposure of features below the WLs is  $1/\#\text{WL}$ . If this is accounted for by addition, the new dose for sufficient exposure becomes  $1 + 1/\#\text{WL}$ , i.e., the parenthesis on the right hand side of Eq. (1).

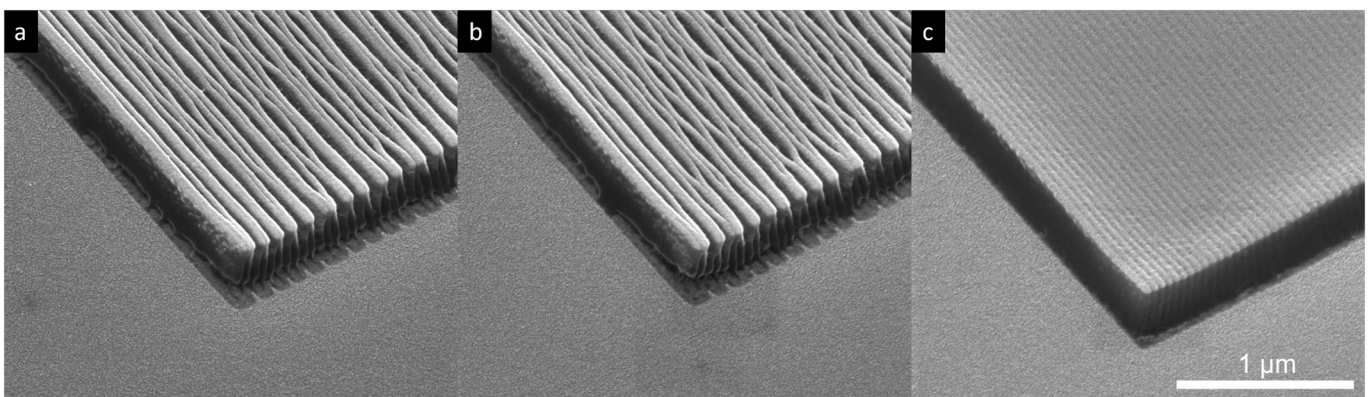


**Fig. 6.** Gratings of the same period (60 nm) as written, with increasing bias, at the same dose of  $286 \mu\text{C}/\text{cm}^2$  ( $1.3 \times 220 \mu\text{C}/\text{cm}^2$ ,  $220 \mu\text{C}/\text{cm}^2$  being the base dose) on 410 nm CSAR 62. The bias goes from 18 nm in (a), to 20 nm in (b) and finally 22 nm in (c). Consequently, there are two WLs per grating line in (a) and (b), and a single WL in (c).

The applicability of the model boils down to understanding that a number of neighbouring WLs will have an impact on each other's exposure. The extent of the influence is setup-dependent, and can easily be determined by looking at the PSF (understood experimentally by considering single-WL writing, as shown in Fig. 9), and by how much it extends past its centre throughout the resist. Implementing this line of thought, a certain #WL may be interpreted as the correct starting point for the model, given the mutual contribution to exposure by said group of WLs to points centred below them, and dose may be ramped up according to Eq. (1) thereafter. Let this point be 10 WLs, and let the area dose for writing 10 WL-structures be known. Then, the step-wise increasing dose factor that needs to be implemented at lower #WL (by multiplication with the area dose for 10 WLs) is depicted in Fig. 7.

Note that the above model is heuristic, in that it is derived conceptually and verified experimentally, as shown in Fig. 8. Eq. (1) estimates well the dose conversion from Fig. 8a to Fig. 8c, where 5 and 4 WLs produce underdosed structures, respectively. It is likewise successful at translating the dose in Fig. 8b to the one in Fig. 8d, where 5 and 4 WLs achieve even structures, respectively. Application of the correction proposed in Eq. (1) thus enables EBL of structures with 5 WLs and 4 WLs alike. By extension, features of different sizes may be dosed sufficiently. For context, to have dosed sufficiently means that edge features will not be poorly developed: it is accounted for that exposure cone edges naturally receive less energy than the cone's centre because of how exposure is spread by the PSF.

The model may be seen as the successor to a previously reported dose compensation scheme [3]. It was proposed that an appropriate dose correction would be given by multiplication with the ratio of old-to-new area of exposure. Even though a change in area likely leads to a need for change in dose, it would do so indirectly, as it would imply a change in WL count, and it is this which then causes dose to be allocated differently. The novelty in our model is found in its capability to account for drastic and sudden demands in dose-change for areas that are close in size. The ramp-up in dose occurs in discrete steps, wherever a WL is gained or lost, rather than being smoothly determined by a change in the exposure area.

A typical PEC procedure involves computations for the PSF [4], and accounting for it in the allocation of dose throughout an area of exposure [5,6]. Simulations require in-depth knowledge of the resist, which might not be available, and their outcome may lose rigor. It is thus convenient to have a model as in Eq. (1) to fall back to, which has been shown to solve dose insufficiency (see Fig. 8) with little to no assumptions.

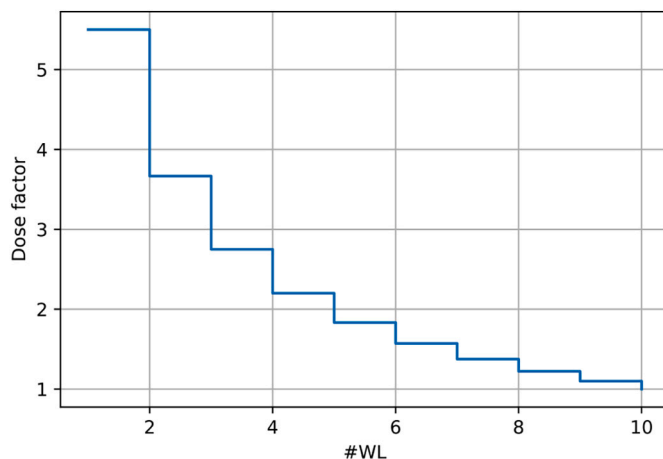


Fig. 7. Visualisation of the increase in dose factor that is necessary to achieve write-through of reduced WL count-features. 10 WLs are chosen as the correction starting point (below which the dose factor is increased) and the step-wise increase follows the model in Eq. (1).

### 3.4. Limit of setup and model

Having established how the EBL tool interprets an area element (assigning to it however many WLs fit according to LS), and having understood dose loss because of downsizing, it becomes relevant to test the limit of the instrumentation. This consists of attempting to write the smallest possible pattern; if it were specified as an area element, then it would have to be at least LS-wide and below  $2 \times LS$ , such that a single WL may be allocated. Alternatively, the EBL tool could be programmed to write by SPLs, to which appropriate line doses would have to be assigned. These two writing schemes must be equivalent, as our arguments for dose insufficiency are based on understanding how WLs are allocated; equivalence would show that our interpretation is correct. Simple geometry, following Fig. 2, gives that conversion from area to line dose boils down to a multiplication by SS, as written in Eq. (2).

$$\text{Area Dose} = \text{Line Dose} \cdot \text{SS} \quad (2)$$

Fig. 9 showcases gratings that were obtained by Au electroplating post EBL of 5 nm area elements (a) or SPLs (b) for the realisation of 80 nm period gratings. Knowing that  $SS = 5$  nm, it can be appreciated how Eq. (2) gives a perfect conversion from one dose to the other, hence equivalence of the two writing schemes.

It is worth mentioning that, to further corroborate our understanding of the WL allocation scheme, the writing of area elements that were thinner than LS was tested and resulted in no dose allocation at all; no feature was written as no WL could be assigned by the VOYAGER.

### 3.5. Towards an elegant EBL scheme

Whilst the limit of the EBL tool is plain, the resolution limit of the procedure is another matter. The fact that the dose that is necessary for write-through is understood does not translate to the possibility of writing features of any size and at any pitch. Going back to the issue of forward scattering, beam broadening takes its toll on closely packed features, and feature collapse may occur. Ultimately, resolution at the bottom of the resist layer is given by the PSF in combination with development contrast. These explain how energy is taken in the resist, and how edges of the cones of exposure become blurred in post-EBL chemistry, respectively. Provided that sufficient dose is given for write-through of cone edges, adjacent features cannot present overlapping cones, otherwise no resist wall would exist between them after development.

Implementation of bias and thus feature downsizing implies dose ramp-up as proposed by our model. Added dose means more energy being deposited at the edges of the exposure cone, which results in broader structures. One inevitably faces a trade-off: for the smallest and most well-defined feature, should biasing be implemented further or halted, resulting in dose ramp-up or no ramp-up, respectively? Finding the optimal amount of WLs for writing concise features in a given resist layer could be the basis for another study.

One should thus think about sizes when planning EBL, and only aim for the realisation of what the WLs allow. Note that LS does not have to be as large as 5 nm, as chosen for proving the principle of our model. If this is reduced, more WLs coexist in a confined area, and the correction in Eq. (1) becomes smoother. Regardless, the model can readily be implemented as soon as the group of mutually dose-contributing WLs is understood.

What remains to be discussed is how the arguments that have been raised, leading to the formulation of our model, translate for cases that implement other resist thicknesses. The majority of our work is based on coping with the effects of forward scattering. Assuming that one writes on resist layers that are so thin that such scattering does not disturb exposure-adjacent regions, it follows that no corrections are necessary. On the contrary, corrections are crucial when beam broadening in the resist is wide enough that when partitioning dose between WLs, the broadening from one WL stretches significantly past the neighbouring

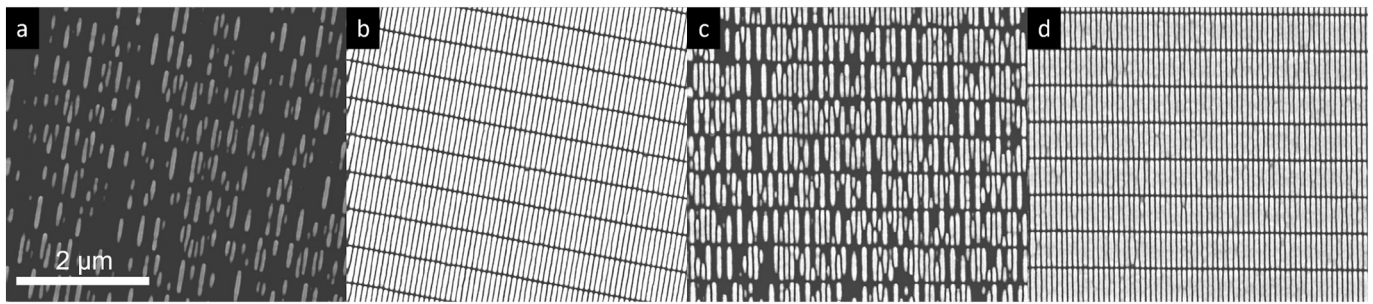


Fig. 8. 80 nm period gratings obtained by the exposure of 40 nm-wide area elements that were biased by 15 nm (a and b) or 20 nm (c and d), resulting in the actual exposure of 25 nm and 20 nm lines, respectively. The area doses were: 245  $\mu\text{C}/\text{cm}^2$  (a); 270  $\mu\text{C}/\text{cm}^2$  (b); 290  $\mu\text{C}/\text{cm}^2$  (c); 320  $\mu\text{C}/\text{cm}^2$  (d).

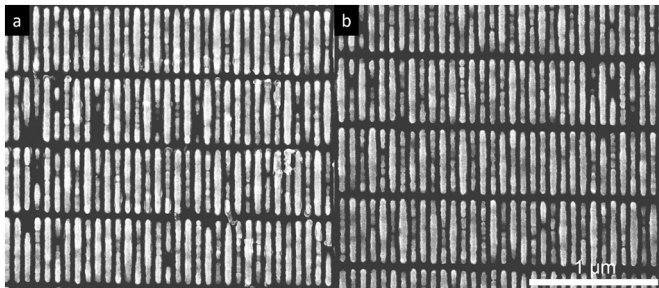


Fig. 9. Comparison of the results from writing with area elements that are 5 nm (one WL) wide (a) and SPLs (b). These were implemented in the realisation of Au gratings of 80 nm period; the former required 812.5  $\mu\text{C}/\text{cm}^2$  and the latter 406.25  $\mu\text{C}/\text{cm}^2$  for resist write-through.

WL. It is in this case that the loss of a WL will truly impact overall dosage: the thicker the resist layer, the greater the overlap of the cones of exposure from neighbouring WLs, hence the more relevant the loss of a WL becomes. It follows that our model applies best when attempting to correct for write-through in thick resist layers; the model is instead expected to fail for very thin resist layers, where the intake of dose by the resist occurs mainly due to single scattering events from the impinging e-beam, hence no contribution from forward-scattered electrons and write-through stays vertical. The same arguments may be raised for different e-beam acceleration voltages: high voltage means less scattering and low means more. The combination of resist thickness and voltage makes each experiment unique and the applicability of the model has to be investigated by the user.

#### 4. Conclusion

We have investigated the phenomenon of dose insufficiency that arises when reducing the size of features within an EBL pattern, specifically, when the widths of the latter are close to the resolution limit of the lithography tool. We have understood that the leading cause for this is the loss of WLs, and have formulated a model that is capable of providing an expectation value for appropriate dosage of some area of exposure based on the number of WLs that fit within it. It was possible to efficiently fabricate tall nanostructures with the combination of 50 kV EBL and CSAR 62 resist. Based on our results, it could be confirmed that our model is applicable to the writing of downsized gratings, and may thus be implemented in further studies. It would grant the possibility of producing features of different sizes within the same EBL pattern without having to run dose-tests prior to the final experiment. This is particularly interesting as it has been reported that conventional PEC

has failed in such an application [7], and patterning required local PEC considerations. The above, together with the model's simplicity and applicability without many requirements, are some practical advantages that make it very attractive. Furthermore, the model helps to develop a deeper understanding for EBL. Topics treated in this paper are often hidden, or taken for granted, in reports of procedures for nano-fabrication by EBL, yet it is important to comprehend how dose allocation takes place: should a PEC user encounter issues with the corrections suggested by some software, they would more readily know how to tackle the issue by knowing how corrections should take place.

#### Declaration of Competing Interest

The authors declare that they have no known competing financial interests or personal relationships that could have appeared to influence the work reported in this paper.

#### Acknowledgements

This research was funded by the Swedish Research Council grant number 2018–04237 and 2019–06104.

#### References

- [1] N. Pala, M. Karabiyik, *Electron beam lithography (ebl)*, in: B. Bhushan (Ed.), *Encyclopedia of Nanotechnology*, Springer, Netherlands, Dordrecht, 2016, pp. 1033–1057.
- [2] Z. Zhou, *Electron beam lithography*, in: Y. Nan, Z.L. Wang (Eds.), *Handbook of Microscopy for Nanotechnology*, Springer, US, 2005, pp. 287–321.
- [3] E. Seo, O. Kim, Dose and shape modification proximity effect correction for forward-scattering range scale features in electron beam lithography, *Jpn. J. Appl. Phys.* 39 (2000) 6827–6830.
- [4] P. Hudek, D. Beyer, Exposure optimization in high-resolution e-beam lithography, *Microelectron. Eng.* 83 (2006) 780–783.
- [5] M.C. Rosamond, J.T. Batley, G. Burnell, B.J. Hickey, E.H. Linfield, High contrast 3d proximity correction for electron-beam lithography: an enabling technique for the fabrication of suspended masks for complete device fabrication within an uhv environment, *Microelectron. Eng.* 143 (2015) 5–10.
- [6] C. Hou, W. Yao, W. Liu, Y. Chen, H. Duan, J. Liu, Ultrafast and accurate proximity effect correction of large-scale electron beam lithography based on fmm and saas, 2020 4th international workshop on advanced patterning solutions, IWAPS 2020 (2020).
- [7] J. Zhu, S. Zhang, S. Xie, C. Xu, L. Zhang, X. Tao, Y. Ren, Y. Wang, B. Deng, R. Tai, Y. Chen, Nanofabrication of 50 nm zone plates through e-beam lithography with local proximity effect correction for x-ray imaging, *Chinese Physics B* 29 (2020), 047501.
- [8] W.W. Molzen, A.N. Broers, J.J. Cuomo, J.M. Harper, R.B. Laibowitz, Materials and techniques used in nanostructure fabrication, *Journal of Vacuum, Sci. Technol.* 16 (1979) 269–272.
- [9] S. Gorelick, J. Vila-Comamala, V. Guzenko, R. Mokso, M. Stapanoni, C. David, Direct e-beam writing of high aspect ratio nanostructures in pmma: a tool for diffractive x-ray optics fabrication, *Microelectron. Eng.* 87 (2010) 1052–1056.
- [10] A.S. Gangnaik, Y.M. Georgiev, J.D. Holmes, New generation electron beam resists: a review, *Chem. Mater.* 29 (2017) 1898–1917.

- [11] I. Kostic, K. Vutova, E. Koleva, R. Andok, A. Bencurova, A. Konecnikova, G. Mladenov, Study on polymers with implementation in electron beam lithography, in: *Polymer Science: Research Advances, Practical Applications and Educational Aspects*, Formatex Research Center, 2016, pp. 488–497.
- [12] M. Schirmer, B. Büttner, F. Syrowatka, G. Schmidt, T. Köpnick, C. Kaiser, M. Schirmer, Chemical semi-amplified positive e-beam resist (csar 62) for highest resolution, *Proc. SPIE* 8886 (2013) 90–96.
- [13] A. Hryciw, Raith GDSII MATLAB Toolbox, University of Alberta, version 1.2, URL, [https://github.com/nrc-cnrc/Raith\\_GDSII](https://github.com/nrc-cnrc/Raith_GDSII), 2014.
- [14] A. Kaganskiy, T. Heuser, R. Schmidt, S. Rodt, S. Reitzenstein, Csar 62 as negative-tone resist for high-contrast e-beam lithography at temperatures between 4 k and room temperature, *Journal of Vacuum Science & Technology B, Nanotechnology and Microelectronics: Materials, Processing, Measurement, and Phenomena* 34 (2016), 061603.
- [15] H. Ohlin, T. Frisk, M. Åstrand, U. Vogt, Miniaturized sulfite-based gold bath for controlled electroplating of zone plate nanostructures, *Micromachines* 13 (3) (2022).
- [16] Université de Sherbrooke, Monte Carlo Simulation of electron trajectory in solids (CASINO), version 3.3.0.4, URL, <https://www.gel.usherbrooke.ca/casino/index.html>, 2016.